

Optical Engineering

OpticalEngineering.SPIEDigitalLibrary.org

Overdrive technology compensating for ambient temperature

Minkoo Kim
Jong-Man Kim
Donggun Lee
Seung-Woo Lee

Overdrive technology compensating for ambient temperature

Minkoo Kim, Jong-Man Kim, Donggun Lee, and Seung-Woo Lee*

Kyung Hee University, Department of Information Display and Advanced Display Research Center, 1 Hoegi-dong, Dongdaemun-gu, Seoul 130-701, Republic of Korea

Abstract. We propose an overdrive (OD) technology to precisely compensate for the temperature-dependent response characteristics of liquid-crystal displays (LCDs). The optical responses of LCDs are highly dependent on ambient temperature. After analyzing the optimized OD values, the new OD technology uses simple calculation logic instead of bulky OD lookup tables to obtain OD values of rising transitions over a wide range of ambient temperatures. We also show that it is possible to automatically adjust the optimum OD values depending on the ambient temperature. The results show that the proposed OD technology can improve motion image quality without any motion artifacts regardless of the ambient temperature. We expect that our proposed OD technology will ensure that LCD products have a consistent motion image quality regardless of the ambient temperature without any increase in cost. © The Authors. Published by SPIE under a Creative Commons Attribution 3.0 Unported License. Distribution or reproduction of this work in whole or in part requires full attribution of the original publication, including its DOI. [DOI: 10.1117/1.OE.54.2.023107]

Keywords: liquid-crystal display; overdrive; ambient temperature; response time.

Paper 141762 received Nov. 13, 2014; accepted for publication Jan. 30, 2015; published online Feb. 25, 2015.

1 Introduction

Liquid-crystal displays (LCDs) have become a universal choice for display applications regardless of their size. LCDs are globally used for peripheral devices of personal computers, large televisions, digital information displays (DIDs), and mobile devices.¹⁻⁴ Therefore, it has become increasingly important to optimize the driving characteristics of LCDs depending on the diverse environments, especially in ambient temperatures. Ambient temperature is one of the most critical factors that directly affect the movement of liquid crystals (LCs). The change in LC movement may result in the degradation of the motion image quality in LCDs. The technology that is often used to handle the LC movement is the overdrive (OD) technology. Conventional OD technology requires several lookup tables (LUTs) and interpolation logics.⁵⁻¹⁰ The LUTs are usually extracted at a fixed temperature, such as room temperature; thus, LCDs are forced to use the fixed OD values regardless of their ambient temperatures. However, applying adequate OD values to the panel depending on ambient temperatures is necessary to maintain optimized moving picture characteristics anywhere and anytime. Figure 1 shows the annual temperature range of selected cities. The average annual temperature difference was $\sim 24^\circ\text{C}$. However, Vladivostok and Beijing showed a temperature difference of $>30^\circ\text{C}$, which could cause severe response performance degradation in LCDs. In this study, we propose a new OD technology that can easily obtain optimum OD values depending on ambient temperatures.

Section 2 of this paper describes a previously proposed OD technology that did not require LUTs. Compensation for the temperature dependency of response characteristics

using twisted-nematic (TN) and fringe-field switching (FFS) LCD panels is described in Sec. 3 of the paper.

2 OD Technology in Our Previous Literature

Figure 2 shows a graphical illustration of the OD concept. Here, G_N is data of gray level and L_N is the target luminance of G_N . As shown in Figs. 2(a) and 2(b), LC responses of transitions from G_1 to G_2 and G_1 to G_3 do not reach the target levels L_2 and L_3 in a frame time (1/60 s), respectively. We can see that the LC response of the transition from G_1 to G_3 reaches L_2 , the target luminance of G_2 , after one frame time as shown in Fig. 2(b). Thus, we can get an ideal luminance response for the transition from G_1 to G_2 if we change the data sequence to be $G_1 \rightarrow G_3 \rightarrow G_2$ rather than $G_1 \rightarrow G_2 \rightarrow G_2$. Here, G_3 is the OD value of the transition from G_1 to G_2 .¹¹

We proposed an OD technology using a third-order approximation in 2010.¹¹ Figure 3 shows the measured OD values for rising transitions of a TN LCD monitor panel at 20°C . In this figure, D_{OD} , D_{PF} , and D_{CF} are the OD data, previous frame data, and current frame data, respectively. Symbols represent the optimized OD values of rising transitions. Each line represents a fitting line over the measured points of rising transitions with a given D_{PF} (0, 32, 64, ..., or 224) in the $(D_{OD} - D_{PF})$ versus D_{CF} space, as shown in Fig. 3. However, if we determine four parameters of a line for a fixed D_{PF} , which we call as a base line, we could easily extract an OD line for transitions with different D_{PF} by shifting the base line. The four parameters of the base line could be obtained by two default points and two measurement points. For example, the default points correspond to a rising transition to white and no transition. In Fig. 4(a), the upper-right blue solid circle represents a rising transition from $D_{PF} = 64$ to $D_{CF} = 255$. Thus, the OD value should be 255. The lower-left blue solid circle represents no transition because D_{PF} and D_{CF} are both 64. The third-order equation

*Address all correspondence to: Seung-Woo Lee, E-mail: seungwoolee@khu.ac.kr

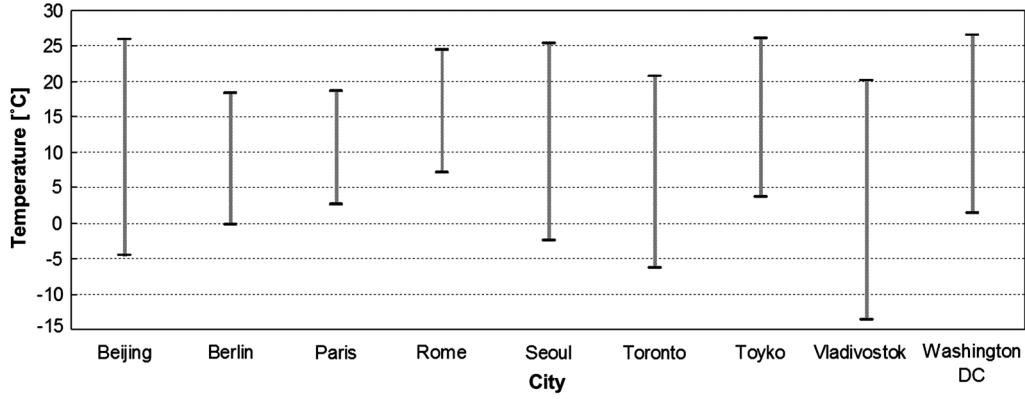


Fig. 1 Annual range of temperatures of some representative cities.

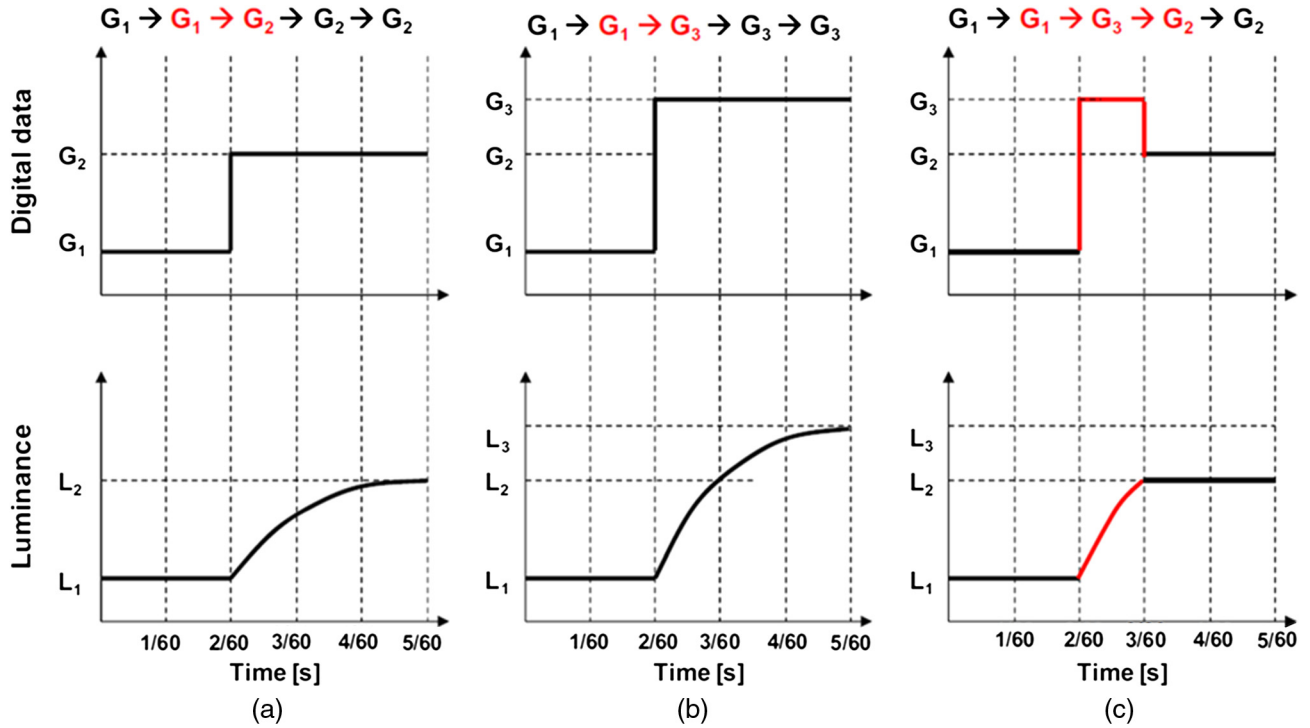


Fig. 2 Concept of overdrive (OD) technology: (a) luminance response of the transition from G_1 to G_2 , (b) luminance response of the transition from G_1 to G_3 , and (c) luminance response when overdrive is applied.

of the base line can then be solved by obtaining only two OD values of two different transitions with $D_{CF} = 128$ and 192 , which are represented by solid red diamonds in Fig. 4(a). By shifting the base line, we could extract whole OD lines, as shown in Fig. 4(a). The third-order equation of the base line is expressed as follows:

$$y = \alpha x^3 + \beta x^2 + \gamma x + C. \quad (1)$$

Here, $x = D_{CF}$ and $y = D_{OD} - D_{PF}$. Four parameters (α , β , γ , and C) are obtained easily because we know the values of the four points of the third-order equation. We shifted the base line to both the x and y directions to obtain a new fitting line for transitions with a different D_{PF} . Then the line with a different D_{PF} can be expressed by Eq. (2). The shift in the x direction, Δx , is dependent on D_{PF} . Δx increases with D_{PF} for rising transitions. Thus, Δx can be expressed by Eq. (3).

The shift in the y direction, Δy , is simply obtained by subtracting the previous frame data of the new fitting line from that of the base line, as shown in Eq. (4).

$$y = \alpha(x - \Delta x)^3 + \beta(x - \Delta x)^2 + \gamma(x - \Delta x) + C + \Delta y, \quad (2)$$

$$\Delta x = \left(\frac{s}{255} \right) \times (D_{PF} - D_{PF_BL}), \quad (3)$$

$$\Delta y = D_{PF_BL} - D_{PF}. \quad (4)$$

Here, s and D_{PF_BL} represent the shifting parameter and the D_{PF} of the base line, respectively. Figure 4(b) shows the results of shifting the base line ($D_{PF_BL} = 64$) to fit the OD lines for the transitions with different D_{PF} conditions. The

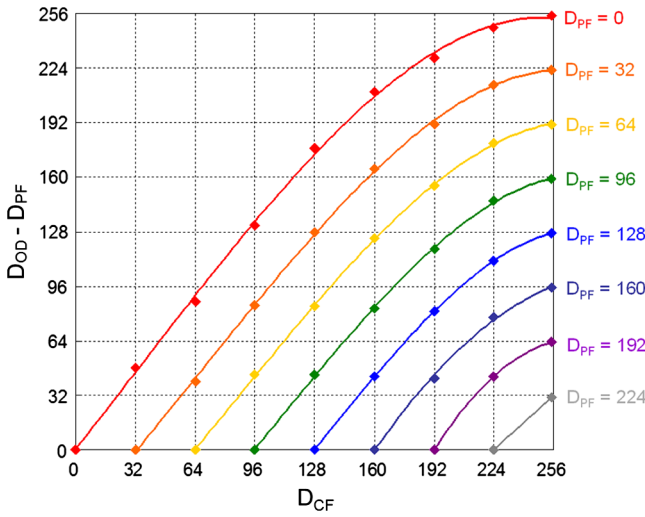


Fig. 3 Relationship among OD values (D_{OD}), previous frame data (D_{PF}), and current frame data (D_{CF}) at 20°C. Symbols are measured data and lines are fitting lines for data of rising transitions with fixed D_{PF} .

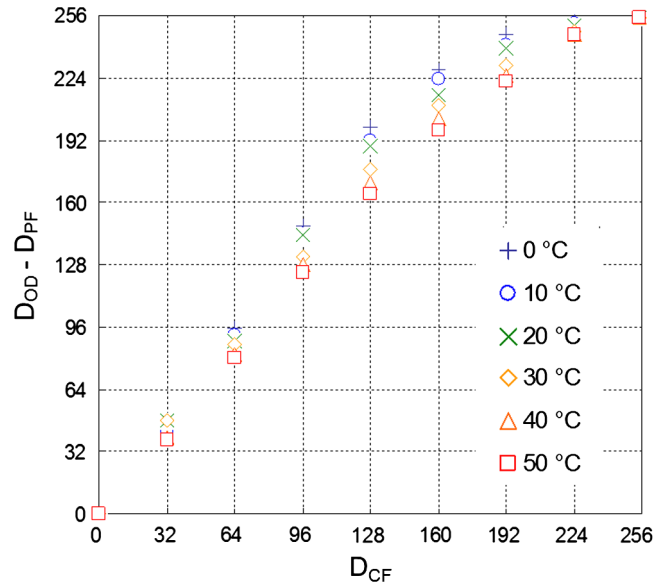


Fig. 5 Results of optimum OD values depending on ambient temperature ($D_{PF} = 0$).

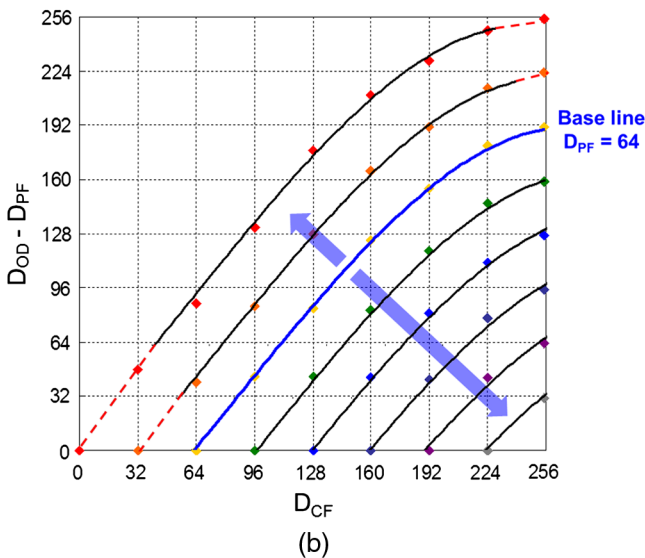
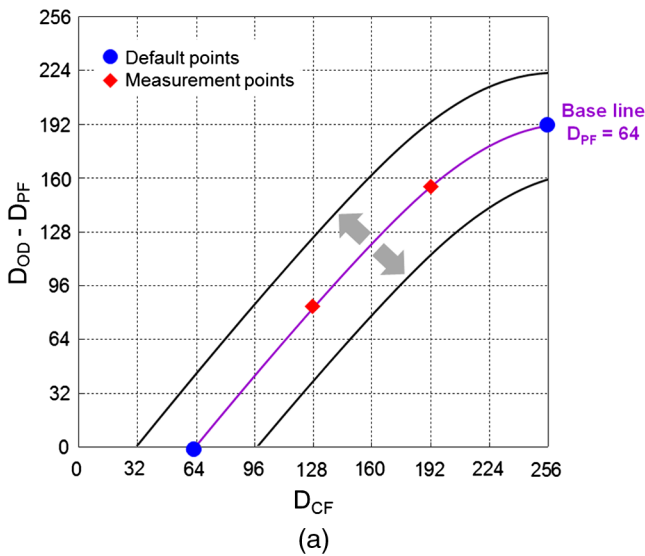


Fig. 4 (a) Graphical illustration for creating and shifting a base line using a third-order approximation. (b) Shifting results when the base line is $D_{PF} = 64$.

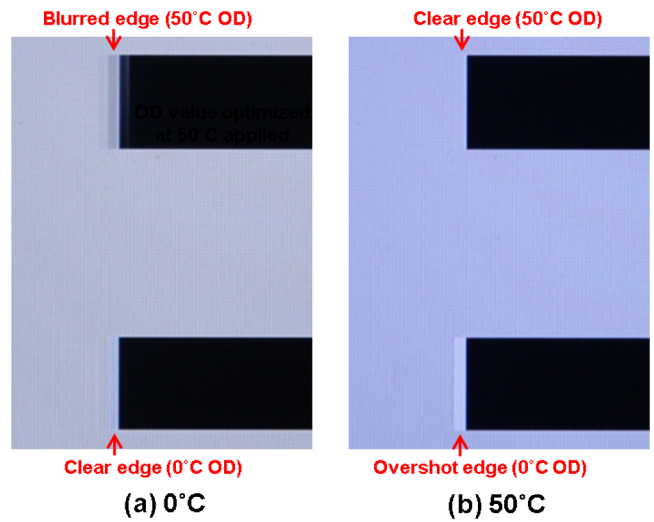


Fig. 6 Photograph of moving bars on fringe-field switching (FFS) liquid-crystal display (LCD) panel operating at (a) 0°C and (b) 50°C.

average deviation of OD approximation by shifting the base line in Fig. 4(b) was 3.50 gray levels.

3 Temperature-Independent TN and FFS LCD Panels

Figure 5 shows the optimized OD values of rising transitions of the TN LCD monitor panel with $D_{PF} = 0$ depending on the ambient temperature between 0 and 50°C. The biggest difference in values of $D_{OD} - D_{PF}$ between 0 and 50°C was 35 gray levels when $D_{CF} = 128$. The average difference was ~20 gray levels. This indicates that visual artifacts, such as overshoot, will be visible if OD values optimized at 0°C are applied to the LCD panel operating at 50°C. Further, moving pictures will have more blurred edges when OD values optimized at 50°C are applied to the panel operating at 0°C.^{12–15} For example, for the data transition from 0 to 192, the FFS LCD panel has optimum OD values of 228 and 197 at 0

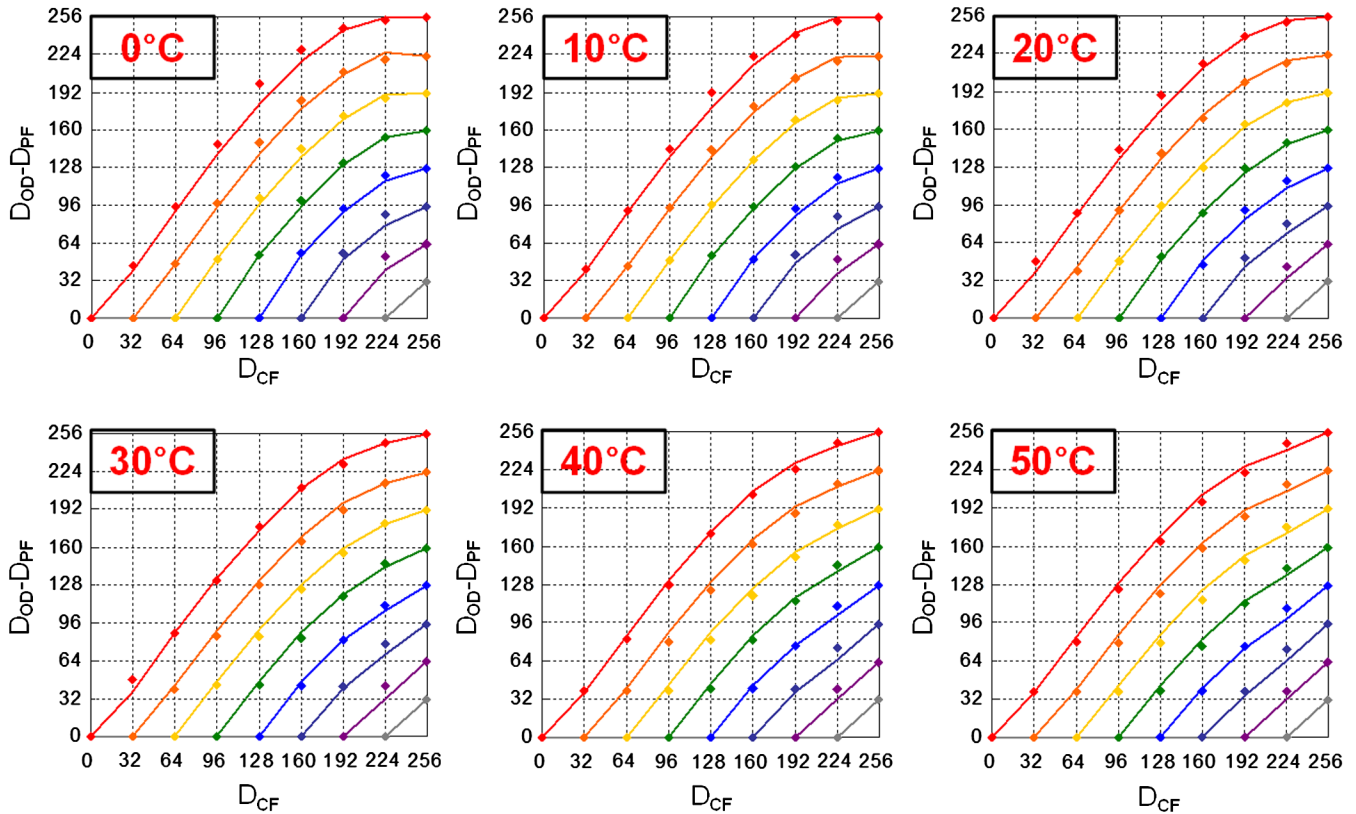


Fig. 7 Application results of γ manipulation to twisted-nematic (TN) LCD panel operating at 0, 10, 20, 30, 40, and 50°C. Here, α and β optimized at 20°C were used, and γ was shifted depending on ambient temperature.

and 50°C, respectively. A moving bar with the different gray level from a background level represents a transition; thus, we can easily observe the motion quality of the transition depending on the OD values applied to the bar. We applied gray levels 197 and 228 as OD values for the upper and lower bars, respectively. We took pictures of the moving bars on the LCD panel operating at 0 and 50°C as shown in Fig. 6. The photograph in Fig. 6(a) was taken when the ambient temperature was 0°C. The upper bar showed the blurred edge and the lower one showed the clear edge as shown in Fig. 6(a). The OD values optimized at 50°C causes the motion blur on the LCD panel operating at 0°C. The photograph in Fig. 6(b) was taken when the ambient temperature was 50°C. The

upper bar showed the clear edge and the lower one showed the overshoot edge as shown in Fig. 6(b). The OD values optimized at 0°C causes the motion artifact, like the brighter overshoot on the LCD panel operating at 50°C. We can conclude that visual artifacts are visible even on the overdriven LCD panel because OD values are very dependent on the ambient temperature. Thus, OD values need to be updated depending on the ambient temperature.

Among the four coefficients (α , β , γ , and C) of the third-order base line, we decided to set the values of α , β , and C ($\alpha = -1.18 \times 10^{-5}$, $\beta = 1.76 \times 10^{-3}$, and $C = -9.67 \times 10^{+1}$) optimized at 20°C. The coefficient γ is manipulated to fit the third-order OD lines optimized at 0, 10, 30, 40, and 50°C.¹¹

Table 1 Optimized coefficients of the third-order approximation of the base line ($D_{PF} = 64$) and averaged deviation at 0, 10, 20, 30, 40, and 50°C [twisted-nematic liquid-crystal display (LCD) panel].

Temperature	Coefficients				Averaged deviation (gray levels)
	α	β	γ	C	
0°C			1.48		4.79
10°C			1.47		3.86
20°C			1.45		3.89
30°C	-1.18×10^{-5}	1.76×10^{-3}	1.43	$-9.67 \times 10^{+1}$	3.54
40°C			1.41		4.36
50°C			1.40		5.18

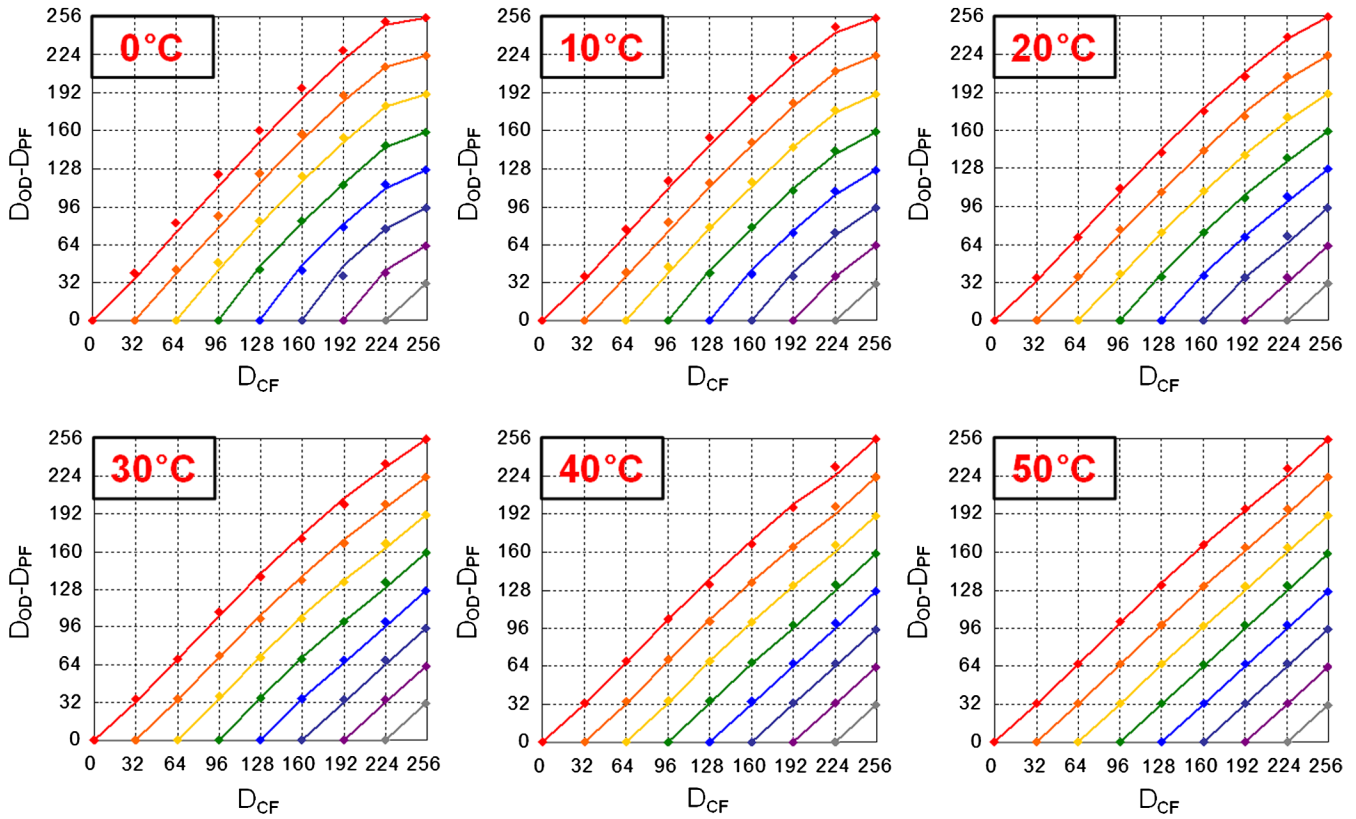


Fig. 8 Application results of γ manipulation to FFS LCD panel operating at 0, 10, 20, 30, 40, and 50°C.

Here, the shifting parameter is set to 64 to minimize the average deviation of the approximation at 20°C. Figure 7 shows the adjustment results of third-order OD lines at 0, 10, 20, 30, 40, and 50°C when using the same α and β values optimized at 20°C and manipulating γ . Table 1 shows optimum coefficients of the third-order approximation for rising transitions at 0, 10, 20, 30, 40, and 50°C when the base line of the TN panel is set to $D_{PF} = 64$. The average deviation of the approximation over six ambient temperatures was 4.27 gray levels, which was acceptable because the average deviation is not far beyond 3.0.¹⁶ The average deviations depending on temperature are listed in Table 1. Table 1 indicates the decrease in γ as the ambient temperature increases.

We applied our proposed method to an LCD monitor panel with FFS mode. As above, we decided to set the values of α , β , and C ($\alpha = -4.46 \times 10^{-6}$, $\beta = 7.86 \times 10^{-4}$, and $C = -7.40 \times 10^{+1}$) optimized at 20°C and manipulate the coefficient γ . The shifting parameter of the FFS LCD panel was set to 22 for best fit. Figure 8 shows the adjustment results of third-order OD lines at 0, 10, 20, 30, 40, and 50°C by using the same coefficients, α and β , obtained at 20°C and manipulating coefficient γ . The average deviation over six different temperatures was 2.79 gray levels, which is more acceptable than that of the TN LCD panel because the deviation is <3 .¹⁶ The average deviations for each temperature are listed in Table 2. The application results over the six

Table 2 Optimized coefficients of the third-order approximation of the base line ($D_{PF} = 64$) and averaged deviation at 0, 10, 20, 30, 40, and 50°C (fringe-field switching LCD panel).

Temperature	Coefficients				Averaged deviation (gray levels)
	α	β	γ	C	
0°C			1.18		4.71
10°C			1.16		3.32
20°C	-4.46×10^{-6}	7.86×10^{-4}	1.13	$-7.40 \times 10^{+1}$	2.07
30°C			1.11		2.39
40°C			1.08		2.29
50°C			1.06		1.93

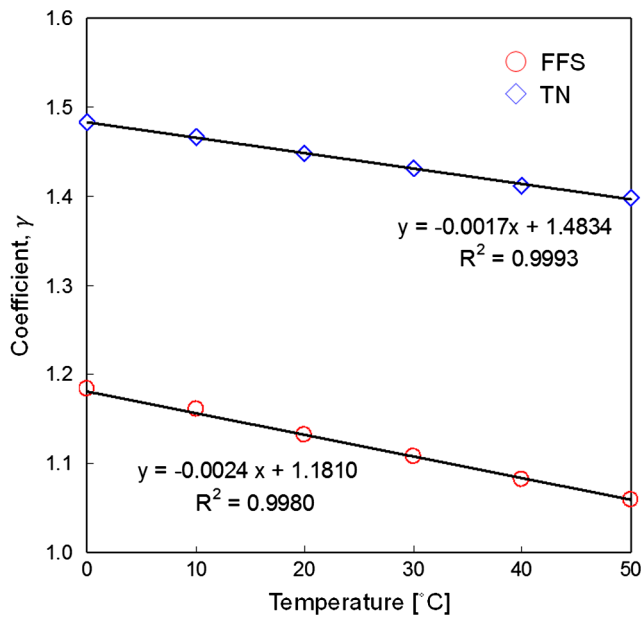


Fig. 9 Relationship between coefficient γ and ambient temperatures (TN and FFS panels).

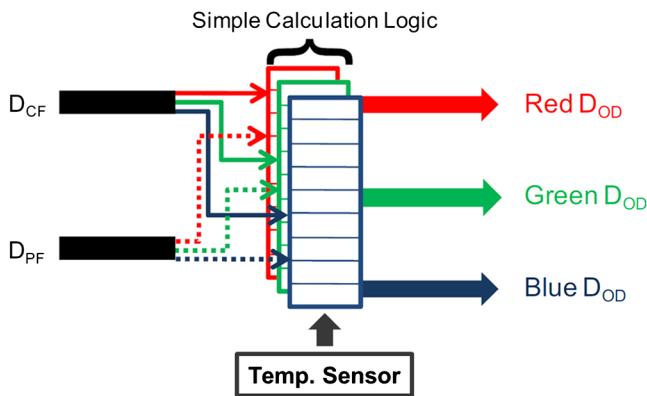


Fig. 10 Proposed hardware architecture to automatically optimize OD values regardless of ambient temperature.

ambient temperatures show that our proposed method with FFS mode has a better performance than with the TN mode. In addition, we also investigated the coefficient γ depending on the ambient temperature. Figure 9 shows a very good linear relationship of the coefficient γ with the ambient temperature for TN and FFS modes. In addition, we expect that the slopes (-0.0017 and -0.0024 for TN and FFS, respectively) can be fixed depending on LC modes and this will be investigated using several LCD panels in the future study.

By applying our proposed method to TN and FFS LCD panels, we found out that the ambient temperature-dependent response characteristics of LCDs could be compensated if the coefficient γ is linearly manipulated according to the ambient temperature. Our new OD implementation technology uses a simple calculation logic in comparison with the bulky LUTs as explained in our previous literature in 2010.¹¹ In addition, it is not difficult to include the value of the slope of the first-order equation in the calculation logic. If a real-time temperature sensor integrated in the LCD panel can provide ambient temperature information for the calculation logic, the LCDs can easily compute optimum OD values,

as shown in Fig. 10. In conclusion, automatically optimizing OD values depending on ambient temperatures is feasible in both TN and FFS LCD panels. In other words, LCDs can automatically optimize OD values of any rising transitions at any ambient temperature if calculation logic memorizes information about the following parameters:

1. α , β , γ , and C of the base line optimized at 20°C (two measurements are needed)
2. Shifting parameter, s (one measurement is needed)
3. The value of the slope for manipulating γ value depending on LC modes.

4 Conclusion

The temperature-dependent response characteristics of LCDs were studied. We proposed a new OD technology to keep the motion image quality of LCDs optimized at any ambient temperature. It has been confirmed that the automatic adjusting of OD values depending on ambient temperatures is practical for both TN and FFS LCD panels. Our technology can be highly useful for mobile applications and DIDs operating in diverse temperature conditions.

Acknowledgments

This work was supported by the Industrial Strategic Technology Development Program (10041596, Development of core technology for TFT free active matrix addressing color electronic paper with day and night usage), funded by the Ministry of Trade, Industry & Energy (MI, Korea).

References

1. S.-W. Lee, "Intelligent liquid crystal display (i-LCD) for next generation television application," *IEEE Trans. Consum. Electron.* **53**(4), 1247–1253 (2007).
2. A. Cellatoglu and K. Balasubramanian, "Autostereoscopic imaging techniques for 3D TV: proposals for improvements," *IEEE J. Disp. Technol.* **9**(8), 666–672 (2013).
3. S. Hong and O. Kwon, "A pixel structure and a simultaneous driving method for high transmittance of transparent digital information displays," *IEEE J. Disp. Technol.* **11**(1), 65–72 (2015).
4. J. Kim and S.-W. Lee et al., "A novel method to accurately predict color information of liquid crystal displays with light leakage from black pixels," *IEEE J. Disp. Technol.* **9**(3), 162–169 (2013).
5. H. Okumura and H. Fujiwara, "A new low-image-lag drive method for large-size LCTVs," *J. Soc. Inf. Disp.* **1**(3), 335–339 (1993).
6. J. Wang and J. Chong, "Adaptive multi-level block truncation coding for frame memory reduction in LCD overdrive," *IEEE Trans. Consum. Electron.* **56**(2), 1130–1136 (2010).
7. S. W. Lee, "Elimination of line dimming artifact in liquid crystal display monitors," *Electron. Lett.* **42**(4), 207–208 (2006).
8. S. W. Lee and H. Nam, "A new dithering algorithm for higher image quality of liquid crystal displays," *IEEE Trans. Consum. Electron.* **55**(4), 2134–2138 (2009).
9. M. O. Tareq, Y. Cho, and S. W. Lee, "A universal implementation method of overdrive in display systems regardless of speed of LCD panels," *SID Symp. Dig. Tech. Pap.* **40**(1), 1259–1262 (2009).
10. Y. Shimodaira et al., "Acceptable limits of gamma for a TFT-liquid crystal display on subjective evaluation of picture quality," *IEEE Trans. Consum. Electron.* **41**(3), 550–554 (1995).
11. Y. Cho et al., "New overdrive technology for liquid-crystal displays with a simple architecture," *Opt. Eng.* **49**(3), 034001 (2010).
12. J. Miseli, "Motion artifacts," *SID Symp. Dig. Tech. Pap.* **35**(1), 86–89 (2004).
13. S. W. Lee, "Contrast enhancement in liquid crystal displays by adaptive modification of analog gamma reference voltages," *ICICE Trans. Electron.* **E90-C**(11), 2083–2087 (2007).
14. Y. Igarashi et al., "Summary of moving picture response time (MPRT) and futures," *SID Symp. Dig. Tech. Pap.* **35**(1), 1262–1265 (2004).
15. S. W. Lee et al., "Motion artifact elimination technology for liquid-crystal-display monitors: advanced dynamic capacitance compensation method," *J. Soc. Inf. Disp.* **14**(4), 387–394 (2006).
16. Y. Cho et al., "Universal overdrive technology for all types of liquid crystal displays," *Opt. Eng.* **50**(3), 034001 (2011).

Minkoo Kim received his BS and MS degrees from the Department of Information Display at Kyung Hee University, Republic of Korea, in 2011 and 2013, respectively. He is currently working toward his PhD degree in the same department at Kyung Hee University. His research interests include driving methods and circuits for various types of displays, including liquid-crystal display (LCD) and OLED.

Jong-Man Kim received his BS and MS degrees in physics and information display at Kyung Hee University, Republic of Korea, in 2010 and 2012, respectively. He is currently working toward his PhD in the Department of Information Display at Kyung Hee University. His research interests include driving methods and circuits for LCD and e-paper displays and driving technology for color motion performance of LCDs.

Donggun Lee received his BS degree from the Department of Information Display at Kyung Hee University, Republic of Korea, in 2015. He is currently working toward his MS degree in the same department at Kyung Hee University. His research interests include driving methods and circuit simulation for LCD and OLED display.

Seung-Woo Lee received his MS and PhD degrees from KAIST in electrical engineering in 1995 and 2000, respectively. He joined Samsung in 2000, where his work has focused on the development of key driving technologies for active-matrix LCDs. He is currently an associate professor in the Department of Information Display at Kyung Hee University. He has been active with SID as a senior member. He became an IEEE senior member in 2010.